





ORIGINAL ARTICLE

Domain-Specific Diaschisis: Lesions to Parietal Action Areas Modulate Neural Responses to Tools in the Ventral Stream

Frank E. Garcea ^{1,2,3,4}, Jorge Almeida ^{5,6}, Maxwell H. Sims¹, Andrew Nunno¹, Steven P. Meyers^{7,8}, Yan Michael Li⁸, Kevin Walter⁸, Webster H. Pilcher⁸ and Bradford Z. Mahon ^{1,2,3,8,9,10}

¹University of Rochester, Department of Brain & Cognitive Sciences, 358 Meliora Hall, Rochester, NY 14627, USA, ²University of Rochester, Center for Language Sciences, 358 Meliora Hall, Rochester, NY 14627, USA, ³University of Rochester, Center for Visual Science, 274 Meliora Hall, Rochester, NY 14627, USA, ⁴Moss Rehabilitation Research Institute, 50 Township Line Road, Elkins Park, PA 19027, USA, ⁵University of Coimbra, Faculty of Psychology and Educational Sciences, Rua do Colégio Novo, Coimbra, 3001-802 Portugal, ⁶University of Coimbra, Proaction Laboratory, Faculty of Psychology and Educational Sciences, Rua do Colégio Novo, Coimbra, 3001-802 Portugal, ⁷University of Rochester Medical Center, Department of Imaging Sciences, 601 Elmwood Avenue, Rochester, NY 14642, USA, ⁸University of Rochester Medical Center, Department of Neurosurgery, 601 Elmwood Avenue, Rochester, NY 14642, USA, ⁹Department of Neurology, University of Rochester Medical Center, 601 Elmwood Avenue, Rochester, NY 14642, USA and ¹⁰Department of Psychology, Carnegie Mellon University, 5000 Forbes Avenue, Pittsburgh, PA 15213, USA

Address correspondence to Bradford Z. Mahon, Meliora Hall, University of Rochester, Rochester, NY 14627-0268, USA. Email: mahon@rcbi.rochester.edu  orcid.org/0000-0002-2018-4797

Abstract

Neural responses to small manipulable objects (“tools”) in high-level visual areas in ventral temporal cortex (VTC) provide an opportunity to test how anatomically remote regions modulate ventral stream processing in a domain-specific manner. Prior patient studies indicate that grasp-relevant information can be computed about objects by dorsal stream structures independently of processing in VTC. Prior functional neuroimaging studies indicate privileged functional connectivity between regions of VTC exhibiting tool preferences and regions of parietal cortex supporting object-directed action. Here we test whether lesions to parietal cortex modulate tool preferences within ventral and lateral temporal cortex. We found that lesions to the left anterior intraparietal sulcus, a region that supports hand-shaping during object grasping and manipulation, modulate tool preferences in left VTC and in the left posterior middle temporal gyrus. Control analyses demonstrated that neural responses to “place” stimuli in left VTC were unaffected by lesions to parietal cortex, indicating domain-specific consequences for ventral stream neural responses in the setting of parietal lesions. These findings provide causal evidence that neural specificity for “tools” in ventral and lateral temporal lobe areas may arise, in part, from online inputs to VTC from parietal areas that receive inputs via the dorsal visual pathway.

Key words: anterior intraparietal sulcus, dorsal stream, fMRI, manipulable objects, neurosurgery, supramarginal gyrus, tools, ventral stream, voxel-based lesion-activity mapping, voxel-based lesion-symptom mapping

Introduction

High-level visual areas in ventral and lateral temporal cortex exhibit a consistent topography by semantic category, with subregions exhibiting neural specificity for places, faces, body parts, tools, and written words (e.g., see Allison et al. 1994; Martin et al. 1996; Kanwisher et al. 1997; Downing et al. 2001; Haxby et al. 2001; Cohen et al. 2002; for review, see Grill-Spector and Malach 2004; Martin 2007; Peelen and Downing 2007; Op de Beeck et al. 2008). On the ventral surface of the temporal lobe, medial regions (e.g., medial fusiform gyrus, collateral sulcus, parahippocampal gyrus) exhibit stronger neural responses for places and large non-manipulable objects than for faces and animals (e.g., see Epstein and Kanwisher 1998; Chao et al. 1999; Downing et al. 2006), while more lateral regions exhibit the reverse profile: stronger responses for animate entities (faces, animals) than nonliving stimuli (e.g., see Kanwisher et al. 1997; Chao et al. 1999; Rogers et al. 2005; Tsao et al. 2006). It is also consistently observed that small manipulable objects, or tools, lead to stronger neural responses than animate entities in medial regions of ventral temporal cortex (faces, animals; e.g., Chao et al. 1999; Noppeney et al. 2006; Mahon et al. 2007; Mahon et al. 2013), but those tool preferences are typically weaker than the responses to places, houses, and large contextualized objects (e.g., see Downing et al. 2006; Chen et al. 2017). Given that places tend to elicit stronger neural responses than tools in medial ventral temporal cortex, in particular anterior medial regions such as the parahippocampal gyrus, many syntheses of category-specificity assume medial ventral temporal regions exhibit specificity for places, “large things”, or contextualized objects (Bar 2004; Downing et al. 2006; Konkle and Oliva 2012) and generally give less consideration to the idea of neural specificity for small manipulable objects or “tools” (e.g., Op de Beeck et al. 2008). That construal of the “categories” of category-specificity in the ventral stream is a legacy of the paradigmatic assumption that the category for which a given subregion exhibits specificity is just that stimulus class that elicits the maximal univariate response (e.g., Downing et al. 2006).

Other lines of investigation have emphasized neural signatures other than the overall amplitude of response in order to argue that there are neural signatures “specific” to “tools” in left posterior ventral medial temporal cortex. For instance, the regions of ventral temporal cortex that exhibit differential responses to tools, compared with faces or animals, also exhibit privileged functional connectivity to the left supramarginal gyrus and anterior intraparietal sulcus (aIPS), regions that support praxis and hand-shaping for object-directed grasping, respectively (e.g., Noppeney et al. 2006; Mahon et al. 2007; Simmons and Martin 2012; Almeida et al. 2013; Garcea and Mahon 2014; Hutchison et al. 2014; Stevens et al. 2015; Hutchison and Gallivan 2016; Chen et al. 2017). Furthermore, in ventral temporal cortex, the voxel-wise pattern of functional connectivity to parietal tool-preferring areas is related to the voxel-wise pattern of tool preferences—indicating a fine-grained alignment between connectivity and stimulus preferences (Chen et al. 2017). Other studies have argued that action-relevant properties of objects drive specialization for “tools” in medial ventral temporal areas (Mahon et al. 2007; see also Valyear and Culham 2010). In summary, while tools may not elicit the strongest overall response in medial ventral temporal cortex, a number of findings indicate that connectivity with parietal action-relevant regions is topographically aligned with regional neural specificity for tools. Those findings collectively motivate what has been referred to (Riesenhuber 2007) as a “connectivity-constrained

account” of the causes of category-specificity in the ventral object processing pathway (Mahon and Caramazza 2011). The core of that proposal is that innately specified connectivity between ventral stream subregions and other parts of the brain provide an initial “scaffolding” that drives the macroscopic organization by semantic category in the ventral stream. That type of theoretical framework has yielded empirical successes in the domains of face (Saygin et al. 2011; Osher et al. 2016) and printed word recognition (Bouhali et al. 2014; Hannagan et al. 2015; Saygin et al. 2016; Stevens et al. 2017) and has spurred proof-of-principle computational simulations (Chen and Rogers 2015). A connectivity-constrained account also provides a natural explanation for why individuals who are congenitally blind show similarly organized patterns of category-specificity in ventral temporal cortex as do sighted individuals (Buckel et al. 1998; Mahon et al. 2009; Striem-Amit et al. 2012; He et al. 2013). However, it is important to emphasize that a connectivity-constrained account of ventral stream organization does not preclude the contribution of other factors to the organization of the ventral stream (e.g., Levy et al. 2001; Tootell et al. 2008; Arcaro et al. 2017).

A connectivity-constrained account of neural specificity for tools in medial ventral regions is a proposal about the principal constraint that shapes the large-scale organization of the ventral stream. A distinct hypothesis can be articulated specifically for the category “tools”: the “specificity” of neural responses to tools in ventral temporal cortex is shaped, online, by inputs from parietal cortex. It is known that the dorsal visual pathway, including the aIPS, has access to semantically uninterpreted information about the location and volumetric properties of graspable objects (Fang and He 2005; Almeida et al. 2008; Almeida et al. 2010; for review, see Binkofski and Buxbaum 2013; Osiurak and Badets 2016; Buxbaum 2017). For instance, Prentiss et al. (2018) showed that a patient with a lower right quadrantanopia could spontaneously orient his wrist during ballistic grasping movements to grasp targets located in the cortically blind field. However, the patient was at chance to make perceptual orientation judgments to the same target stimuli in his cortically blind field—those data (see also Perenin and Rossetti 1996) demonstrate that the dorsal stream can process information about the orientation of an elongated object independent of processing within the geniculostriate pathway (for evidence from visual agnosia, see Goodale et al. 1991). However, in order to generate a functionally appropriate grasp (avoid the sharp end of a knife, or grasp a slippery glass with the appropriate grip force), semantically interpreted information about visual form, surface-texture, and material properties must inform object grasps (e.g., Rosenbaum et al. 1990; Goodale et al. 1994; Carey et al. 1996; Creem and Proffitt 2001). A poignant demonstration of that is visual agnosic patient DF’s inability to grasp visually presented familiar objects in a functionally appropriate manner (despite her ability to grasp them in a volumetrically and biomechanically appropriate manner; e.g., see Carey et al. 1996).

Medial ventral temporal regions represent surface-texture and material properties (Cant and Goodale 2007; Arnott et al. 2008; Cant et al. 2009; Cavina-Pratesi et al. 2010; Gallivan et al. 2014; Stassenko et al. 2014). Thus, by hypothesis, interactions between ventral and dorsal stream regions unfold during the computation of functionally appropriate grasps. A possible function of those interactions would be to winnow the space of biomechanically possible object grasps down to the space of functionally appropriate grasps. Note that while ventral temporal areas likely represent surface and material properties about

non-tools (e.g., animals, furniture, etc.), those classes of stimuli do not engage the dorsal visual pathway. Thus, while surface-texture and material properties may be processed for non-tools in ventral temporal areas, those ventral temporal areas will not (by hypothesis) receive input from parietal action-related areas for those non-tool stimuli. Thus, on the strong form of this view, the “category-specificity” of neural responses to tools in left ventral temporal cortex results, in part, from filters that determine which stimuli the dorsal stream responds to, rather than filters local to the ventral stream itself. This proposal predicts that neural responses for tools in left ventral temporal cortex should be modulated in a domain-specific manner by lesions to parietal areas supporting object-directed grasping.

The goal of the current study was to use causal evidence to test the prediction that lesions to left aIPS disrupt stimulus-evoked neural responses for tools in left ventral temporal cortex. A key control analysis tests whether parietal lesions disrupt neural responses to place stimuli in the same region of left ventral temporal cortex. This is an important and strong control because place stimuli elicit (if anything) stronger neural responses than tool stimuli in ventral temporal cortex (Downing et al. 2006). We also test whether lesions to left aIPS disrupt stimulus-evoked responses to tools in the left posterior middle temporal gyrus, and explore whether the left posterior middle temporal gyrus may serve as a “relay” between ventral temporal cortex and action-relevant areas of parietal cortex.

Methods

Participants

A total of 76 individuals participated in this study. All participants had normal or corrected-to-normal vision, and no prior neurosurgeries. Thirty-five of the participants were in the pre-operative phase of a neurosurgical intervention (14 females; mean age, 47.3 years; SD, 16.4 years). Thirty-four of those 35 patients were native English speakers. The etiology of the lesions in the neurosurgery participant group included astrocytoma ($N = 10$), glioma ($N = 9$), glioblastoma ($N = 7$), oligodendroglioma ($N = 3$), mesial temporal lobe sclerosis/temporal lobe epilepsy ($N = 2$), arteriovenous malformation ($N = 2$), and cavernoma ($N = 2$; see Supplementary Table 1). Twenty-five patients had left hemisphere lesions and 10 patients had right hemisphere lesions. The remaining 41 participants (out of the overall group of 76) were healthy adult volunteers (21 female; mean age, 21.2 years; SD, 2.32 years); 3 healthy participants' data were removed due to excessive head motion during the fMRI scans (>2 SD of motion in either translation or rotation in X,Y,Z dimensions), leaving 38 individuals included in the healthy control group. Healthy adult participants were right-hand dominant (as established with the Edinburgh handedness questionnaire), had normal or corrected-to-normal vision, and had no history of neurological disorder. All neurosurgery and healthy adult volunteers participated in the study in exchange for payment, and gave written informed consent in accordance with the University of Rochester Research Subjects Review Board. The results obtained from the neurosurgery patients were used in each case to assist surgical planning to preserve eloquent cortex (e.g., see Garcea et al. 2017; Chernoff et al. under review).

General Experimental Procedure

Stimulus presentation was controlled with “A Simple Framework” (ASF; Schwarzbach 2011) written in MATLAB using the Psychophysics Toolbox (Pelli 1997). All participants viewed the stimuli binocularly through a mirror attached to the head

coil adjusted to allow foveal viewing of a back-projected monitor (temporal resolution = 120 Hz). Each neurosurgery and healthy adult participant took part in several scanning sessions; the data from the first session form the basis for the current investigation. That session consisted of (i) a 6-min T1 anatomical scan; (ii) between 4 and 8 runs of a category localizer experiment (see below for experimental details); (iii) two runs of a 6-min resting state fMRI scan (data not analyzed herein); and (iv) a 15-min diffusion tensor imaging (DTI) scan (data not analyzed herein).

Object-Responsive Localizer Experiment Design

Design and Procedure.

To localize object-responsive areas in the brain, including tool-preferring regions, each participant viewed scrambled and intact images of tools, animals, famous faces, and famous places (for all details on stimuli see Fintzi and Mahon 2014; Chen et al. 2017). Twelve grayscale photographs of tools, animals, faces, and places were used; there were 8 exemplars of each (i.e., 8 different hammers; 8 different pictures of Matt Damon). This resulted in a total of 96 images per category, and 384 total images. Phase-shifted versions of the stimuli were created to serve as a baseline condition. Participants viewed the images in a miniblock design. Miniblock events were 6 or 12 s in duration. Four patients were presented with 6-s miniblocks while 31 patients were presented with 12-s miniblocks. Thirty healthy adult participants were presented with 6-s miniblocks while 8 healthy adults were presented with 12-s miniblocks.

Within each miniblock, 12 stimuli from the same category were presented for 500 ms (6 s miniblock) or 1000 ms (12 s miniblock; 0 ms interstimulus interval), followed by 6 s or 12 s fixation periods (for 6 s and 12 s miniblocks, respectively). Within each run, 8 miniblocks of intact images and 4 miniblocks of phase-shifted versions of the stimuli were presented with the constraint that a category of objects did not repeat during two successive miniblock presentations. Participants who saw 6-s miniblocks took part in 8 runs (91 volumes per run) while participants who saw 12-s miniblocks completed 4 runs (152 volumes per run; for precedent in using this task with neurosurgery patients, see Garcea et al. 2017).

MR Acquisition Parameters

MRI Parameters

Whole brain BOLD imaging was conducted on a 3-Tesla Siemens MAGNETOM Trio scanner with a 32-channel head coil located at the Rochester Center for Brain Imaging. High-resolution structural T1 contrast images were acquired using a magnetization-prepared rapid gradient echo (MP-RAGE) pulse sequence at the start of each participant's first scanning session (TR = 2530, TE = 3.44 ms, flip angle = 7°, FOV = 256 mm, matrix = 256 × 256, 1 × 1 × 1 mm sagittal left-to-right slices). An echo-planar imaging pulse sequence was used for T2*contrast (TR = 2200 ms, TE = 30 ms, flip angle = 90°, FOV = 256 × 256 mm, matrix = 64 × 64, 33 sagittal left-to-right slices, voxel size = 4 × 4 × 4 mm). The first 6 volumes of each run were discarded to allow for signal equilibration (4 volumes during image acquisition and 2 at preprocessing).

Preprocessing of fMRI Data

fMRI data were analyzed with the BrainVoyager software package (Version 2.8.2) and in-house scripts drawing on the BVQX

toolbox written in MATLAB (<http://support.brainvoyager.com/available-tools/52-matlab-tools-bvxqtools/232-getting-started.html>). Preprocessing of the functional data included, in the following order, slice scan time correction (sinc interpolation), 3D motion correction with respect to the first volume of the first functional run, and linear trend removal in the temporal domain (cutoff: two cycles within the run). Functional data were registered (after contrast inversion of the first volume) to high-resolution deskulled anatomy on a participant-by-participant basis in native space. For each participant, echo-planar and anatomical volumes were transformed into standardized space (Goebel et al. 2006). All functional data were smoothed at 6 mm FWHM (1.5 voxels) and interpolated to 3 mm³ voxels. The general linear model was used to fit beta estimates to the experimental events of interest. Experimental events were convolved with a standard 2-gamma hemodynamic response function. The first derivatives of 3D motion correction from each run were added to all models as regressors of no interest to attract variance attributable to head movement.

Lesion Identification

Lesions were identified by visually segmenting healthy cortical tissue from lesioned tissue visible on the native T1 anatomy. Each patient's T1 anatomical dataset was then transformed to Talairach space, and the transformation matrices were applied to the lesion mask to bring it into Talairach space. Lesion masks were confirmed by a neuroradiologist (author S.P.M.) blinded at the time of his analysis to the goals of the study; lesion confirmation made use of all clinical scans available for each patient (e.g., FLAIR, T2, DWI). We then converted each lesion ROI into a whole-brain mask in which voxels associated with a lesion were labeled with a "1" and voxels that were not associated with the lesion were labeled with a "0". Masks were interpolated to a voxel size of 3 mm³ to align with the voxel size of the fMRI data (for lesion coverage, see Supplementary Fig. 1).

ROI Definition: Tool Preferring Left Ventral Temporal Cortex

In both the neurosurgery group and healthy adult group we localized left ventral temporal tool preferring areas at the single-subject level. Spherical seed regions (6 mm diameter) were centered on the peak voxel in each participant, in each region. Left ventral temporal tool-preferring areas were identified with the whole-brain contrast of "Tools > [Animals, Faces, & Places]" (equally weighted). If "Tools > [Animals, Faces, & Places]" did not elicit differential BOLD contrast in left ventral temporal cortex in a particular subject, the threshold was relaxed (to a maximum of $P < 0.05$, uncorrected). In instances in which we could not identify a left ventral tool-preferring peak at a more liberal threshold (i.e., $P < 0.05$, uncorrected), we used the Talairach coordinate from the group-level map (see Fig. 1 for peak coordinates). In the neurosurgery group, we used the group-level defined peak for 6 participants in whom we were unable to localize the left ventral temporal cortex peak; in the healthy adult group, we used the group-level defined peak for 8 participants in whom we were unable to localize the left ventral temporal cortex peak. We note that the peak Talairach coordinate for the neurosurgery-defined ventral temporal cortex ROI was 3 mm in Euclidean distance from the healthy adult-defined peak, indicating excellent correspondence between the two independent datasets.

Strict independence of criteria for voxel definition and test was applied throughout the analysis pipeline. We defined tool-

preferring voxels in a split-run analysis, in which data from the even runs of the category localizer experiment were used to define tool-preferring voxels, and data from odd runs of the experiment were used to measure BOLD contrast to tool stimuli from those ROIs. This was folded, such that we identified tool-preferring voxels with data from odd runs, and used data from even runs of the experiment to measure BOLD contrast for tool stimuli in those ROIs (see Fig. 1). We then averaged across the two data folds.

Voxel-based Lesion Activity Mapping (VLAM)

We measured tool preferences with the contrast of "Tools > [Animals, Faces, & Places]" (weighted equally), averaging over data folds as described (see "ROI Definition: Tool Preferring Left Ventral Temporal Cortex"). For each participant we obtained a measure of the amplitude of tool preferences in left ventral temporal cortex, and separately quantified lesion volume (number of 3 mm³ voxels lesioned). The Voxel-based Lesion Activity Mapping (VLAM) analysis then proceeded in two steps. In the first step we regressed lesion volume on the vector of tool preferences in left ventral temporal cortex. In the second step we correlated (point biserial correlation), at every voxel of the brain, a binarized vector of lesion presence/absence values (across subjects) with the vector of residual tool preferences in the left ventral temporal cortex (having regressed lesion volume). This pipeline was repeated (see below) using the amplitude of place preferences from the same single-subject defined ventral temporal ROIs. The resulting whole-brain partial correlation maps are plotted in Figure 2A.

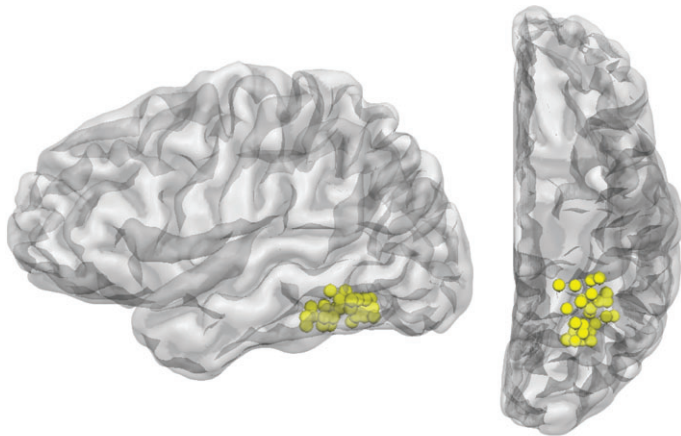
Results

We studied a series of consecutively recruited patients in the pre-operative phase of their neurosurgical care ($n = 35$). Each patient completed the same functional MRI experiment prior to neurosurgery in which they viewed or named gray-scale pictures of tools, animals, famous faces and famous places (for precedent, see Garcea et al. 2017). No patients had lesions extending into the left fusiform gyrus; lesions were distributed throughout anterior (medial and lateral) temporal regions, and parietal and frontal regions (see Supplementary Fig. 1 for a lesion coverage map; see Supplementary Table 1 for lesion etiology). A separate group of healthy participants ($n = 38$) also completed the same fMRI experiment.

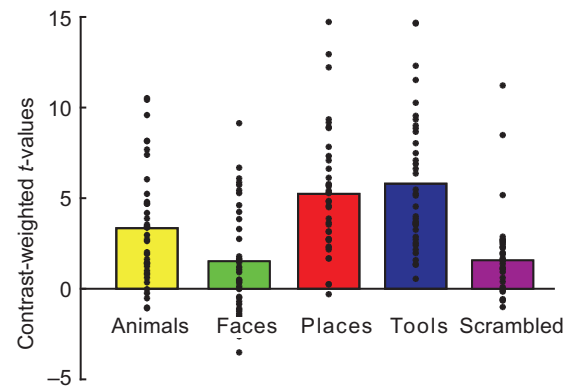
We first established (see Fig. 1) that the neurosurgery and healthy adult group exhibited comparable patterns of category-preferences in left ventral temporal cortex, at the group level. For each participant (healthy adults and neurosurgery patients), half of the data for each participant were used to define a subject-specific peak for tool preferences (using the contrast of "Tools > [Animals, Faces, & Places]" (weighted equally)) and the other half of the data (from that participant) were used to estimate the amplitude of category preferences; this was jackknifed so that both halves of the data for each participant were used for voxel definition and test, and the results were averaged (see Methods for full details). Figure 1 shows the single-subject regions-of-interest (ROI) and also plots the amplitude of category-preferences in left ventral temporal cortex for the healthy adult and neurosurgery participant groups.

A 2_{GROUP} × 5_{CATEGORY} ANOVA was conducted to evaluate whether the pattern of category preferences in ventral temporal tool-preferring regions was comparable across the two groups of participants. There was a main effect of Group ($F(1, 71) = 4.88, P < 0.01$): The patient group had a higher average response across

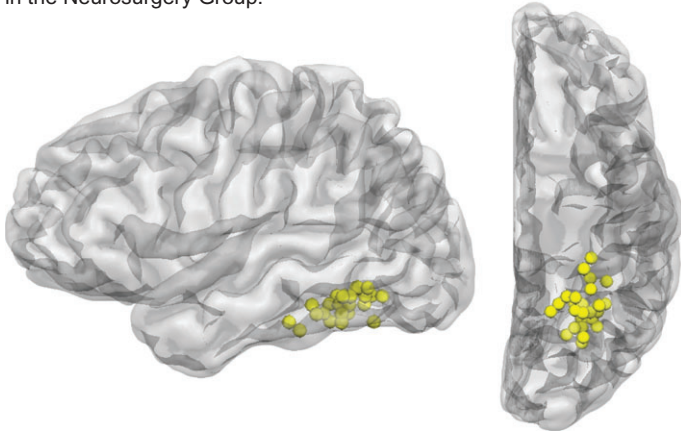
A.i. Left Ventral Temporal Cortex ROIs for Tool Preferences in the Healthy Adult Group.



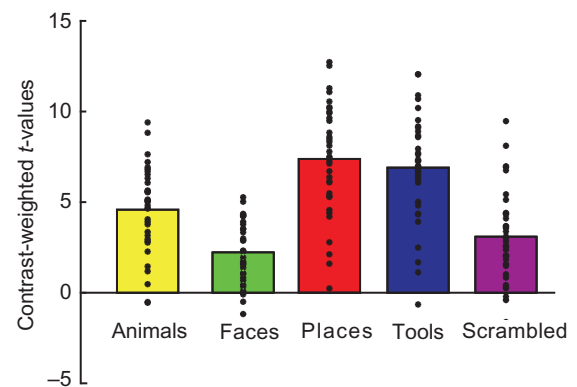
A.ii. Category Responses in the Healthy Adult Group.



B.i. Left Ventral Temporal Cortex ROIs for Tool Preferences in the Neurosurgery Group.



B.ii. Category Responses in the Neurosurgery Group.



 Individual Subject Left Ventral Temporal Cortex Tool Preferring ROI

Figure 1. ROI analysis of ventral temporal tool-preferring voxels. (A) Subject-specific left ventral temporal tool-preferring ROIs are represented as spheres (6 mm diameter). Subject-specific tool-preferring ROIs were defined using half of the data (e.g., even runs) from each participant, and the remaining half the data (i.e., odd runs) from that participant were used to calculate category-preferences at the single-subject level (with averaging across the data folds). The average location for the neurosurgery participant group (mean Talairach X, Y, Z: -27, -55, -17) was in close proximity (Euclidean distance, 3 mm) to the average location in the healthy adult group (mean Talairach X, Y, Z: -27, -58, -17). Plotted in the bar graphs are contrast-weighted t-values for each category versus the fixation baseline. (B) The amplitude of category preferences in single-subject tool-preferring ventral temporal cortex ROIs were obtained in the neurosurgery group (using half of the data to define, the other half to measure). Plotted in the bar graphs are contrast-weighted t-values for each category versus the fixation baseline. Dots in all bar graphs represent individual participants.

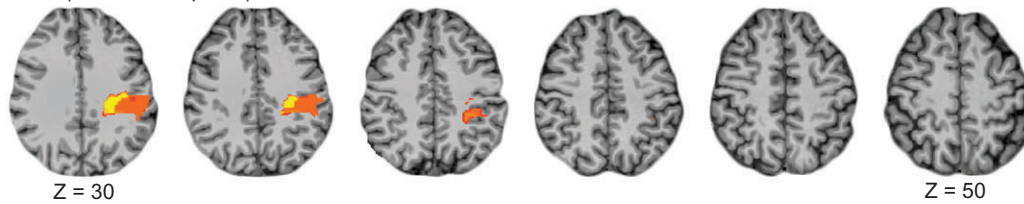
categories than healthy adults (average t-values: patients = 4.84, SEM, 0.25; healthy adults = 3.49, SEM, 0.26; t-values corresponded to each category versus the baseline condition). There was also a main effect of Category ($F(4, 284) = 150.80, P < 0.001$): Consistent with prior results, famous place and tool stimuli elicited the strongest responses in medial ventral temporal cortex (e.g., see Downing et al. 2006; see Fig. 1). In the neurosurgery group, BOLD responses in left ventral temporal cortex were marginally stronger for places than for tools ($t(34) = 1.76, P = 0.08$; see Fig. 1B). In the healthy control group we observed higher amplitude responses for tools than for places ($t(37) = 2.19, P < 0.05$). That divergence in the relative amplitude of tools and places across the two groups led to a marginal interaction between Group and Category ($F(4, 284) = 2.40, P = 0.07$; see Fig. 1). These findings indicated reliable definition of tool preferences in medial ventral temporal cortex in both the healthy controls

and neurosurgery patients; we return below to consider the implications of the (marginal) discrepancy in the amplitude of tool and place preferences in the healthy controls and neurosurgery patients.

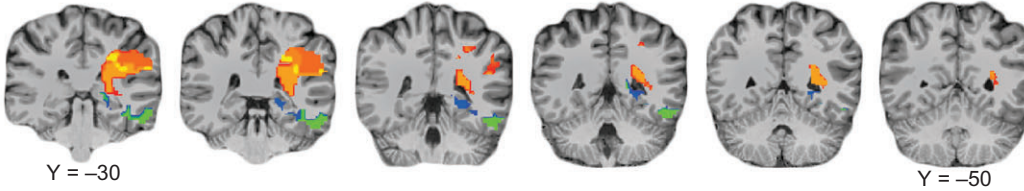
Lesions to aIPS modulate tool preferences in ventral temporal cortex. The key empirical hypothesis to be tested is that tool preferences in left ventral temporal cortex will be modulated by lesions to regions of parietal cortex that support object-directed grasping and manipulation, in particular, left aIPS. To test this hypothesis in an unconstrained manner, we adapted a well-known analytic approach, Voxel-based Lesion Symptom Mapping (VLSM) for use with fMRI. In traditional VLSM (e.g., see Bates et al. 2003), each patient in the group contributes a lesion mask in standard space (e.g., Talairach space; Talairach and Tournoux, 1988); the analysis then relates the presence or absence of a lesion at each voxel to variability across patients

A. Voxelwise correlation between stimulus preferences in left ventral temporal cortex and lesion presence.

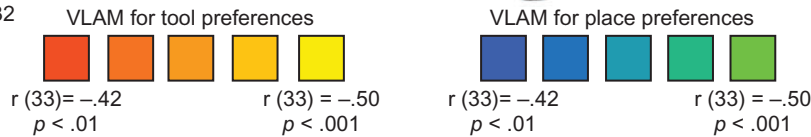
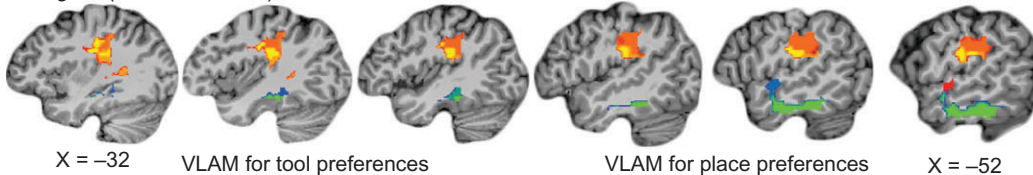
i. Axial (inferior-to-superior)



ii. Coronal (anterior-to-posterior)

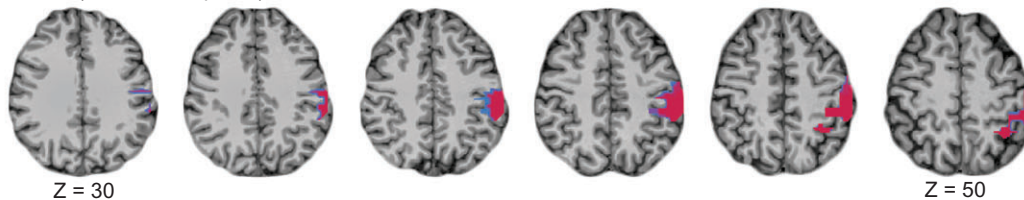


iii. Sagittal (medial-to-lateral)

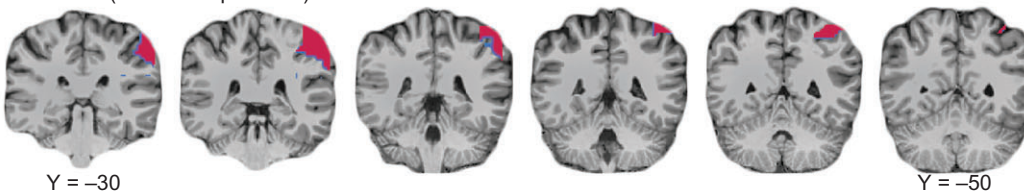


B. Voxelwise comparison between VLAM results for tools and places identifies significant differences in correlation magnitudes in the left aIPS and supramarginal gyrus.

i. Axial (inferior-to-superior)



ii. Coronal (anterior-to-posterior)



iii. Sagittal (medial-to-lateral)

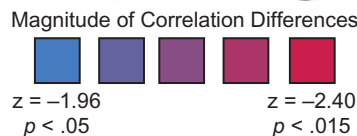
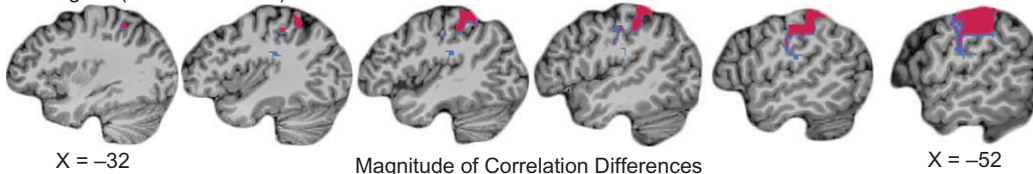


Figure 2. Voxel-based Lesion Activity Mapping (VLAM) showing that lesions to aIPS modulate neural responses to tools in left ventral temporal cortex. (A) Lesions to the left supramarginal gyrus and left anterior intraparietal sulcus, and adjacent white matter areas, are inversely related to tool preferences in left ventral temporal cortex (red-to-yellow color-scale). All partial correlation coefficient values plotted in the map (regressing lesion volume) survive cluster correction (cluster correction using AlphaSim, minimum cluster size of 66 voxels, with an initial alpha level of $P < 0.01$, uncorrected). To test for the specificity of parietal lesions modulating tool responses in left ventral temporal cortex, we repeated the analysis using place preferences as measured from the same tool-preferring ventral temporal ROIs (again, regressing lesion volume). The results, plotted on the blue-to-green color-scale, identify temporal lobe regions but importantly do not identify parietal areas (all

on a reference behavioral task. The resulting group map plots lesion density as a function of performance on the reference neuropsychological task.

In a Voxel-based Lesion Activity Mapping (VLAM) analysis, fMRI-based measures of neural activity in a reference region (in this case, left ventral temporal cortex) are substituted for performance on a behavioral task. In the VLAM analysis as applied herein, the fMRI-based measure was the amplitude of tool preferences, and the reference region was left medial ventral temporal cortex. Thus, across the group of patients, at each voxel in the brain, the presence or absence of a lesion was correlated (point biserial correlation) with tool preferences in left ventral temporal cortex. Tool preferences were estimated by calculating (for each participant) the contrast weighted t -value for the contrast of “[Tools > Animals, Faces, & Places]”, within subject-specific ventral temporal cortex ROIs (using a split-half on the data for voxel definition and test, see Methods). These analyses were conducted both with and without first regressing lesion volume from the vector of category-preferences; the results were unaffected by the variable of lesion volume. All results are reported having regressed lesion volume from the predictor of category preferences.

The core finding that emerged from the VLAM analysis is that tool preferences in left ventral temporal cortex were inversely related to the likelihood of a lesion to left aIPS (Fig. 2A, red-to-yellow color scale). Specifically, lesions to left aIPS were associated with weaker tool preferences in left ventral temporal cortex (Fig. 2A). This finding was robust to the baseline used to calculate tool preferences (e.g., “[Tools > [Animals and Faces]”]; “[Tools > [Scrambled Images]”]; see Supplementary Fig. 2 for details). The fact that the core finding is robust to the baseline used to calculate tool preferences reinforces the inference that lesions to parietal cortex modulate neural responses to tools per se, rather than to other stimuli used as a baseline against which to compute tool preferences.

Parietal modulations of ventral temporal cortex are domain-specific. An important alternative interpretation of our core finding is that neural responses in ventral temporal cortex, potentially to “any” stimulus, are modulated by inputs from parietal cortex. For instance, it could be that connectivity between the left parietal lobule and left fusiform gyrus is important for how ventral temporal cortex responds “generally” to a visual stimulus. One argument against this alternative is that the core finding described above (see Fig. 2A) is observed when relating lesion location to tool “preferences”, i.e., tool responses compared with responses to animals, faces, and places. Nonetheless, it is important to seek decisive evidence against the alternative account that would propose “domain-general” parietal-to-fusiform modulation. That alternative interpretation would predict that neural responses to place stimuli would also be modulated by lesions to left aIPS. To test this prediction, we repeated the VLAM analysis using place preferences rather than tool preferences as the predictor of lesion density (whole-brain analysis, also regressing lesion volume from place preferences). Place preferences were estimated by calculating the contrast-weighted t -values for “[Places > [Animals + Faces + Tools]” (weighted equally), using the same subject-specific ventral temporal ROIs as used for the

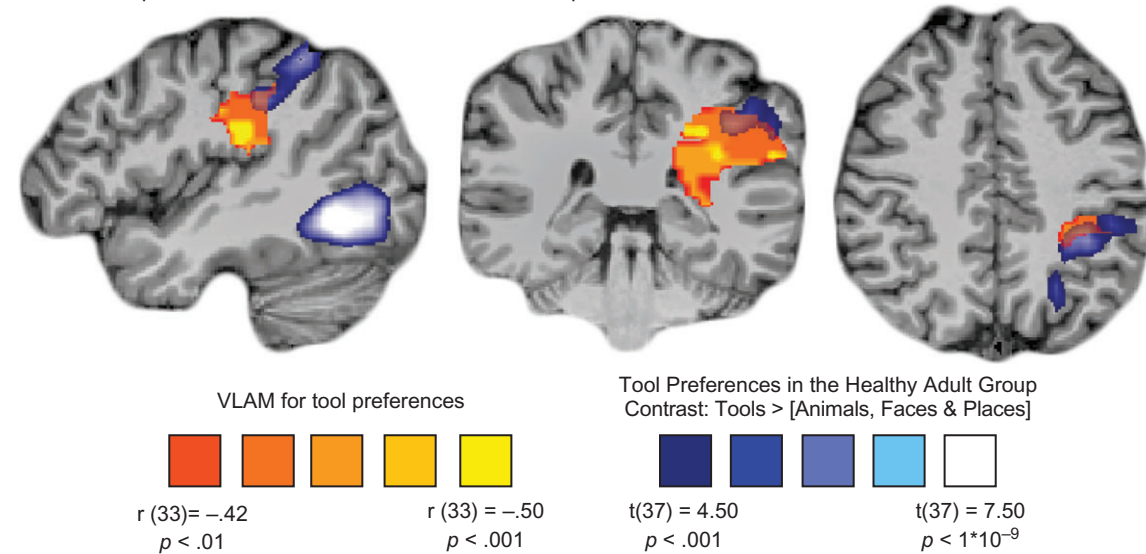
analysis of tool-preferences. The results are plotted on the blue-green color scale in Figure 2A—those analyses did not identify any voxels in parietal cortex but did identify regions in the anterior temporal lobe. Finally, it is also important to emphasize that parietal cortex was not identified when different baselines were used for calculating place preferences (e.g., “[Places > [Animals + Faces]”]; “[Places > [Scrambled Images]”]; see Supplementary Fig. 2 for details). Those control analyses constitute a strong test of the domain-specificity of the core phenomenon because, as noted above (e.g., see Fig. 1B), the overall amplitude of place preferences is (if anything) stronger than tool preferences in left ventral temporal cortex in the neurosurgery group (see Fig. 1).

We next sought to test whether the VLAM results for tools, identifying left parietal cortex, are statistically stronger for tools than for places. To carry out that analysis, we Fisher-transformed the whole-brain maps obtained from the tool and place VLAM analyses, and for each voxel, compared the magnitude differences of the Fisher-transformed correlation coefficients using a z -test. Plotted in Figure 2B are z -values indicating the anatomical locations where VLAM effects for tools were significantly greater than VLAM effects for places (minimum z value, 1.96, $P < 0.05$, uncorrected). Critically, this analysis identifies regions in and around the left aIPS and supramarginal gyrus, as identified in the VLAM analysis in Figure 2A. By contrast, the regions of anterior temporal cortex identified in the VLAM analysis for places were not significantly stronger for places than they were for tools. These findings indicate that the effect of lesions to left parietal cortex on tool responses in left medial ventral temporal cortex was significantly stronger than the effect of lesions to parietal cortex on places preferences in the same medial ventral ROIs.

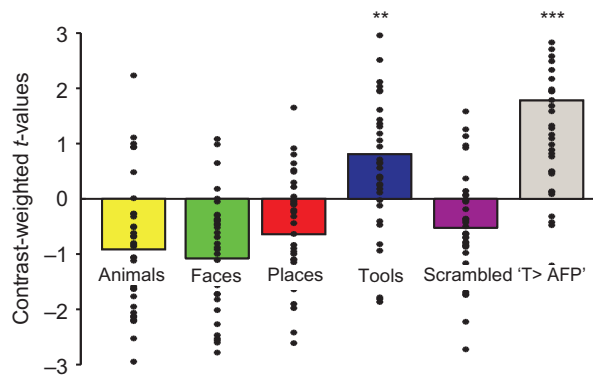
Independent confirmation that the VLAM analyses identify left aIPS. We then sought to confirm that the peak of lesion overlap from the core analysis (Fig. 2A) was in fact in left aIPS, using 3 independent approaches. First, we used the search term “anterior intraparietal” in Neurosynth to estimate the stereotactic coordinates for aIPS (70 studies were identified). A spherical ROI (6 mm diameter) was centered on the resulting coordinate (Talairach X, Y, Z: $-47 -30 38$); using that literature-defined ROI, we then tested for the relation between lesion presence (to that ROI) and tool preferences in ventral temporal cortex. That analysis confirmed a significant relation between lesion presence in the (Neurosynth defined) left aIPS and tool preferences in left ventral temporal cortex ($r(33) = -0.35$, $P < 0.05$). Second, we used that literature-defined ROI of aIPS to measure category-preferences in the healthy adult participants who completed the same fMRI experiment as the patient group. The results demonstrated robust tool responses (“Tools > [Fixation baseline]”, $t(37) = 2.75$, $P < 0.01$), and tool preferences (“Tools > [Animals, Faces, & Places]” (weighted equally), $t(37) = 6.14$, $P < 0.001$; see Fig. 3B). Third, in the healthy adult dataset we carried out a split-half analysis in which we used half of the data to define tool preferences in a whole-brain contrast (“Tools > [Animals, Faces, & Places]” (weighted equally)), and computed the overlap between that whole-brain map and the VLAM-identified parietal voxels shown in Figure 2A. We then

values survive cluster correction, with a minimum cluster size of 68 voxels, initial alpha of $P < 0.01$, uncorrected). The same results were obtained when not regressing lesion volume, and when measuring tool- and place-preferences using alternative baselines (see Supplementary Fig. 2). (B) A direct comparison of VLAM results for tools and those for places identifies the left aIPS and supramarginal gyrus. Plotted in Figure 2B are negative z -values (greater VLAM effect for tools than places; minimum z value = -1.96 , $P < 0.05$, two-tailed). We note that there were no sites associated with VLAM effects for places that were significantly greater than VLAM effects for tools.

A. The overlap between VLAM-identified left aIPS and tool preferences.



B. Amplitude of responses in the left anterior intraparietal sulcus using NeuroSynth-derived coordinates.



C. Amplitude of responses in the left anterior intraparietal sulcus using split-half analysis.

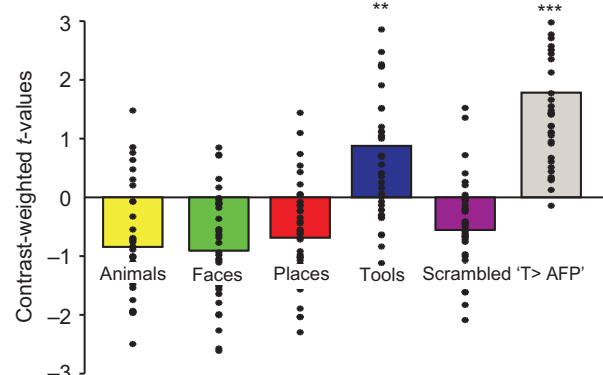


Figure 3. Confirmation that the VLAM analysis identifies the tool-preferring aIPS in the healthy adult group. (A) The overlap between the Voxel-based Lesion Activity Mapping (VLAM) analysis (red-to-yellow color-scale) and tool preferences (Tools > [Animals, Faces, & Places]) (weighted equally) in the healthy adult group (blue-to-white color-scale) was computed. Overlap was maximal at the left aIPS. (B) We independently defined the left aIPS using NeuroSynth and created an aIPS sphere centered on the peak Talairach coordinate (XYZ = -47 -30 38, 6 mm in diameter). Category-preferences for that ROI were extracted for the healthy adult group, and are plotted in the bar graph. The results indicate robust tool responses (one-sample t-test versus fixation baseline, $t(37) = 2.75$, $P < 0.01$) and tool-preferences (“Tools > [Animals, Faces, Places]” (“T > AFP”), $t(37) = 6.14$, $P < 0.001$). (C) In a final test, we extracted category-preferences from the healthy participants for the ROI defined as overlapping the VLAM analysis and tool-preferences in the healthy participants, using a split-half analysis to maintain independence of voxel definition and test. Specifically, using the healthy adult dataset we computed the whole-brain contrast of “Tools > [Animals, Faces, & Places]” using half the data (e.g., even runs) and determined overlap between that map (FDR corrected, $q < 0.05$) and the VLAM results; category-preferences were extracted for voxels identified as overlapping, using the left-out half of data (i.e., odd runs) from the healthy participants (to estimate category-preferences). This procedure was repeated using the other half of the healthy data to define a whole-brain map of tool preferences (e.g., odd runs) and extracting data for the left-out half (i.e., even runs). The results are plotted in the bar graph and demonstrate nearly the exact pattern obtained using the NeuroSynth coordinates for aIPS. There were robust tool responses (one-sample t-test versus fixation baseline, $t(37) = 3.34$, $P < 0.01$) and tool-preferences (“Tools > [Animals, Faces, Places]” (“T > AFP”), $t(37) = 7.78$, $P < 0.001$). Note that the aIPS region identified by the overlap analysis was anatomically proximal (odd runs, 7 mm Euclidean distant; even runs, 7.3 mm Euclidean distant) to the NeuroSynth-defined left aIPS peak, indicating that a common set of anatomical voxels are identified by independent methods for identifying the left aIPS. Dots in the bar graphs represent individual participants. ** = $P < 0.01$; *** = $P < 0.001$.

measured the amplitude of category-preferences for those overlapping voxels using the left-out half of the data from the healthy participants (this procedure was jackknifed and the results were averaged to derive a final measure of category-preferences that maintained independence of voxel definition and test). Again, we observed robust tool responses (“Tools > [Fixation baseline]”, $t(37) = 3.34$, $P < 0.01$), and tool preferences (“Tools > [Animals, Faces, & Places]” (weighted equally), $t(37) = 7.78$, $P < 0.001$; see Fig. 3C). While the overall area of overlap is modest (see Fig. 3 caption for details), the strength of the finding lies in its specificity—both in the specificity of the effect for

tools compared with places, and the anatomical specificity whereby left aIPS is identified through otherwise unconstrained whole-brain analyses. Thus, and taken together, these three sets of converging findings indicate that the VLAM analysis independently identifies, in addition to adjacent white matter in left parietal cortex, tool preferring left aIPS.

General Discussion

We have reported causal evidence that neural responses to tool stimuli in ventral temporal cortex are modulated by inputs

from left aIPS, a region of parietal cortex that supports hand shaping during object-directed grasping. Our core finding is not a general effect of parietal lesions dampening neural responses to “any” stimulus class in the fusiform gyrus, because the amplitude of place preferences in ventral temporal cortex was unrelated to lesions in parietal cortex. This pattern of findings is an instance of what Price, Friston and colleagues (Price et al. 2001; for review, see Price and Friston 2002; see also Carrera and Tononi 2014) have referred to as dynamic diaschisis: The process by which neural responses for a class of stimuli can be disrupted due to disruption of connected but anatomically distant regions. We refer to the pattern of results we have reported as an instance of “domain-specific” diaschisis, in that the pattern of parietal-to-fusiform interactions is constrained by a content-defined domain or stimulus class.

Bar and colleagues (Bar 2003, 2004; Kveraga et al. 2007; for review see Bar 2003; Bar et al. 2006; see also Fintzi and Mahon 2014), argued that orbitofrontal regions process a “gist” or “first-pass” visual representation of an object via fast but low-acuity magnocellular projections. Bar and colleagues argued the “gist” representation is used to guide slower but more detailed analysis by ventral temporal regions (see also Price and Devlin 2004; Bouhali et al. 2014; Hannagan et al. 2015). We suggest that a similar phenomenon may occur for visually presented graspable objects—dorsal stream structures with projections to parietal cortex receive visual information about objects bypassing the geniculostriate pathway, potentially via pulvinar or geniculate projections to MT/V5, or direct geniculate projections to extrastriate regions (e.g., see Sincich et al. 2004; Schmid et al. 2009; Lyon et al. 2010). The dorsal visual pathway has access to perceptually rich (Konen and Kastner 2008; Freud et al. 2016; Kastner et al. 2017) but semantically uninterpreted information (e.g., see Almeida et al. 2008; Almeida et al. 2014). Thus, the dorsal stream has access to volumetric properties such as size, location and orientation of a grasp target, and there is also evidence that elongated objects may enjoy a privileged status in terms of processing within the dorsal stream (e.g., Sakuraba et al. 2012; Almeida et al. 2014; Chen et al. 2018b). This means that aIPS could represent semantically-uninterpreted information about an elongated grasp target prior to, and in parallel to, processing of the object within the geniculostriate pathway (Culham et al., 2003; Konen, Mruzek, Montoya, & Kastner, 2013).

It is known that surface-texture and weight information is processed in ventral medial temporal lobe regions (Cant and Goodale 2007; Cant et al. 2009; Gallivan et al. 2014) and that those types of object information must, at some level of processing, inform functional object grasps. For instance, the manner in which an object is grasped for functional use takes into account not only “bottom-up” or semantically uninterpreted volumetric information (processed in the dorsal visual pathway) but also information about the relevant parts of the object that must be grasped to enable subsequent functional use (Rosenbaum et al. 1990; Creem and Proffitt 2001), as well as its surface and material properties (compare the grip force applied to a wet and soapy glass versus the same glass when dry (for discussion see Mahon and Wu 2015)). By hypothesis, medial ventral temporal lobe regions process surface-texture and material properties about all types of objects (i.e., not just “tools”). However, elongated and graspable objects will also be processed through dorsal stream pathways, in parallel to analysis in the geniculostriate pathway for surface-texture and material properties. Thus, according to the proposal we advance here, ventral temporal cortex exhibits neural specificity for “tools”

because of the satisfaction of two constraints: (i) the object is graspable and thus independently drives processing in the dorsal visual pathway, and (ii) surface-texture and weight information is processed by ventral stream regions. The proposal is not that parietal inputs to ventral temporal regions are “top-down”—but rather that part of the ventral visual hierarchy incorporates inputs from independent analyses propagated through the dorsal visual pathway (analogous to the proposal by Bar 2003).

A recent fMRI study from Chen and colleagues (Chen et al. 2018b) has demonstrated there is asymmetric functional connectivity between left ventral temporal cortex and left anterior IPS. Chen and colleagues used dynamic causal modeling to model the directionality of connectivity among the left medial fusiform gyrus, left posterior middle temporal gyrus, left anterior IPS, and the left superior parietal lobe. They found that the left posterior middle temporal gyrus, but not the left medial fusiform gyrus, exhibits bidirectional functional connectivity with the left anterior IPS during tool processing. Convergent evidence for that inference is provided by the recent study by Garcea and colleagues (Garcea et al. 2018), in which participants performed, in one set of runs, an *n*-back picture matching task, and in another set of runs, an object pantomime task. Critically, both of the tasks were performed over the same stimulus materials and using the same presentation parameters—thus, any differences between the tasks are attributable to the task as opposed to lower-level sensory stimulation. In line with the results of Chen and colleagues (2018b), Garcea and colleagues observed that the left posterior middle temporal exhibited a high degree of network centrality during both the object pantomime task and *n*-back style picture matching tasks and exhibited increased functional connectivity to the left aIPS and left ventral temporal cortex (left medial fusiform gyrus).

While there is evidence for a white matter pathway connecting ventral temporal areas with the left posterior and superior parietal lobule (e.g., see Kravitz et al. 2011; Kravitz et al. 2013; see also Rushworth et al. 2006), we are not aware of evidence of a direct white matter pathway connecting medial ventral tool preferring regions and left anterior IPS; thus, an important possibility is that the left posterior middle temporal gyrus forms an intermediary region between left ventral temporal cortex and left aIPS. That proposal about the role of the left posterior middle temporal gyrus can be initially tested through re-analysis of our data reported herein, in that tool preferences in that region should also be modulated by lesions to left aIPS. We tested this prediction in two ways.

First, in a manner identical to the VLAM analysis of the left ventral temporal cortex (Fig. 2), we localized the left posterior middle temporal gyrus and tested the relation between tool preferences in that region and lesion likelihood, throughout the brain. The left posterior middle temporal gyrus was localized using the same split-half single-subject approach, including data folding (see Methods). We observed that lesions to the left aIPS, left supramarginal gyrus, adjacent white matter inferior to the aIPS, and left lateral and anterior temporal lobe were associated with weaker responses to tools in the left posterior middle temporal gyrus (see Supplementary Fig. 3).

Second, we carried out a “reverse VLAM” analysis. For that analysis, we correlated the vector of aIPS lesion presence (1 s or 0 s corresponding to lesion presence or absence, respectively) with each voxel’s (whole-brain) tool preferences (contrast: “Tools > [Animals, Faces, & Places]” (weighted equally)). This analysis identifies where tool preferences are modulated by the presence of a lesion to the left aIPS. Consistent with our original VLAM analyses (see Fig. 2), we observed that tool

A. Tool preferences in left ventral and lateral temporal cortex are related to aIPS lesions

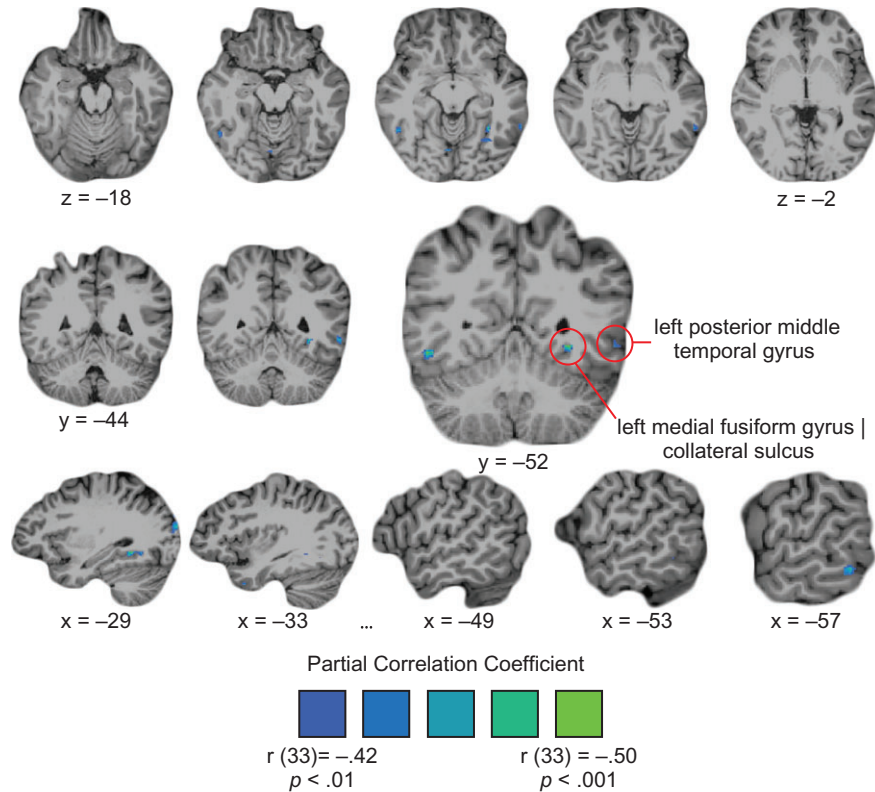


Figure 4. Reverse Voxel-based Lesion Activity Mapping (VLAM) demonstrates tool preferences in left ventral temporal cortex and the left posterior middle temporal gyrus are modulated by left aIPS lesions. (A) A reverse VLAM analysis was carried out in which a vector of aIPS lesion presence/absence was correlated with voxelwise tool preferences (“Tools > [Animals, Faces, & Places]” (weighted equally)) to identify regions (whole-brain) in which aIPS lesions modulate tool preferences. These analyses identify voxels in the left medial fusiform gyrus (collateral sulcus), replicating prior findings (Fig. 2), and also the left posterior middle temporal gyrus. In addition, we found that tool preferences in the right posterior middle/inferior temporal gyrus were modulated in the presence of left aIPS lesions (all correlation values are significant at an alpha level of $P < 0.01$, uncorrected). Note the reverse VLAM maps are plotted in radiological convention.

preferences in left medial ventral temporal cortex (specifically, at the fundus of the collateral sulcus) were inversely related to the likelihood of aIPS lesions (see Fig. 4). Interestingly, and consistent with the idea that left posterior middle temporal gyrus serves as a relay (Chen et al. 2018b), we also observed that tool responses in the left posterior middle temporal gyrus were inversely related to the likelihood of lesions to aIPS (Fig. 4). These findings provide initial support for the proposal that the left posterior middle temporal gyrus modulates connectivity between the left aIPS and left medial ventral tool preferring regions. However, future hypothesis-driven research will be needed to decisively test that proposal—ideally in a focal lesion model using VLAM analyses to understand the long-distance functional implications of lesions at different points within the network of regions involved in tool recognition, grasping and use.

A key issue that is framed, but left open, by the current investigation concerns the nature of the inferior parietal neural representations interface with ventral stream representations of object form, surface-texture, and material properties. We have motivated and interpreted our findings from the perspective of functional object grasping, and in the setting of a “visually” presented object. However, praxis, or the ability to manipulate an object correctly to fulfill its function, is represented in the adjacent supramarginal gyrus, and praxis representations can certainly be accessed for an object that is “in

hand but out of sight” (Kellenbach et al. 2003; Boronat et al. 2005; Canessa et al. 2008; Peeters et al. 2013; Chen et al. 2018a). The VLAM analyses we reported identified white matter structures underlying the left inferior parietal lobule, and the analyses conducted with reference to the left posterior middle temporal gyrus specifically identified the left supramarginal gyrus. In order to access the correct praxis representation, the system must have access to semantically interpreted information about object identity, visual form, and function; and likely, along with access to those types of representations, the system will have accessed surface-texture and material properties. As suggested by Chen and colleagues (2018b), it may be that the posterior middle temporal gyrus serves as a critical hub or relay that allows for cross-modal integration between the dorsal and ventral streams. Future work that utilizes high spatial and temporal resolution neural data (e.g., electrocorticography; see e.g., Caruana et al. 2017) has the potential to disambiguate the degree to which the left posterior middle temporal gyrus exhibits bidirectional (or unidirectional) influences upon the left aIPS and left ventral temporal cortex during tool recognition and use. In that regard, it will be important to relate measures of functional coupling between ventral and dorsal stream regions to performance in tool recognition and real object use (for relevant review and discussion, see Snow et al. 2011; Brandi et al. 2014; Macdonald and Culham 2015; Freud et al. 2017).

Conclusion

The category of tools is a stimulus class that is defined in part by action- or motor-relevant dimensions. An object is a tool, in part, because it is used in a certain manner to fulfill a specific function, commensurate with behavioral goals. We suggest that neural responses to tools in ventral temporal cortex are driven, in part, by the “interpretation” of the object as a motor-relevant object, which is supported by grasp-related areas such as aIPS. The integration of the “interpretation” of a tool as a graspable object with processing of its surface-texture and material properties is reflected, we suggest, in functional connectivity between aIPS and regions in medial ventral temporal cortex. On this account, neural responses to tools in ventral temporal cortex reflect the joint constraint imposed by processing of the stimulus as both a graspable object (via the dorsal stream) and as an object with particular material characteristics that need to be considered to calibrate an object-directed action. This suggested framework brings an account of the causes of category-specific organization in the ventral stream (namely, a connectivity-based account; e.g., Mahon and Caramazza 2011) into register with a processing model of the causes of category-specificity in neural responses. The proposal that the connectivity of the system drives category-specific organization in the ventral stream may extend to other categories (for empirical support, see Saygin et al. 2011; Bouhali et al. 2014; Hannagan et al. 2015; Saygin et al. 2016; Stevens et al. 2017). However, it may be that for other categories, visual information is sufficient to drive, online, category-specific responses (but see Price et al. 2001 for evidence of long-range modulation of responses to printed words in the context of dynamic diaschisis). More broadly, this type of approach emphasizes how multi-sensory integration supports visual categorization, and how connectivity of ventral temporal regions with other brain regions can be instrumental to visual categorization (Martin 2006; Gaillard et al. 2006; Behrmann et al. 2007; Thomas et al. 2009; Yeatman et al. 2013; Thiebaut de Schotten et al. 2014; Ishibashi et al. 2016; Saygin et al. 2011, 2016; Almeida et al. 2018).

Supplementary Material

Supplementary material is available at *Cerebral Cortex* online.

Notes

We are grateful to all individuals who participated in these studies, many of whom were preparing for an upcoming neurosurgery. This research was supported by NIH grants R21NS076176 and R01NS089069 and NSF grant BCS-1349042 to B.Z.M., a core grant to the Center for Visual Science (P30 EY001319), and support to the Department of Neurosurgery at the University of Rochester by Norman and Arlene Leenhouts. Preparation of this ms was supported by a University of Rochester Center for Visual Science pre-doctoral training fellowship (NIH 5T32EY007125-24) to F.E.G. and by a Moss Rehabilitation Research Institute postdoctoral training fellowship (NIH 5T32HD071844-05). J.A. is supported by the Foundation for Science and Technology of Portugal and Programa COMPETE grant (PTDC/MHC-PCN/0522/2014). *Conflict of Interest:* The authors declare no competing financial interests

References

- Allison T, McCarthy G, Nobre A, Puce A, Belger A. 1994. Human extrastriate visual cortex and the perception of faces, words, numbers, and colors. *Cereb Cortex*. 4:544–554.

- Almeida J, Amaral L, Garcea FE, Aguiar de Sousa D, Xu S, Mahon BZ, Pavão Martins I. 2018. Visual and visuomotor processing of hands and tools as a case study of cross talk between the dorsal and ventral streams. *Cogn Neuropsychol*. 24:1–16.
- Almeida J, Fintzi AR, Mahon BZ. 2013. Tool manipulation knowledge is retrieved by way of the ventral visual object processing pathway. *Cortex*. 49:2334–2344.
- Almeida J, Mahon BZ, Caramazza A. 2010. The role of the dorsal visual processing stream in tool identification. *Psychol Sci*. 21:772–778.
- Almeida J, Mahon BZ, Nakayama K, Caramazza A. 2008. Unconscious processing dissociates along categorical lines. *Proc Natl Acad Sci U S A*. 105:15214–15218.
- Almeida J, Mahon BZ, Zapater-Rabero V, Dziuba A, Cabaco T, Marques JF, Caramazza A. 2014. Grasping with the eyes: the role of elongation in visual recognition of manipulable objects. *Cogn Affect Behav Neurosci*. 14:319–335.
- Arcaro MJ, Schade PF, Vincent JL, Ponce CR, Livingstone MS. 2017. Seeing faces is necessary for face-domain formation. *Nat Neurosci*. 20:1404–1412.
- Arnott SR, Cant JS, Dutton GN, Goodale MA. 2008. Crinkling and crumpling: an auditory fMRI study of material properties. *Neuroimage*. 43:368–378.
- Bar M. 2003. A cortical mechanism for triggering top-down facilitation in visual object recognition. *J Cogn Neurosci*. 15: 600–609.
- Bar M. 2004. Visual objects in context. *Nat Rev Neurosci*. 5: 617–629.
- Bar M, Kassam KS, Ghuman AS, Boshyan J, Schmid AM, Dale AM, Halgren E. 2006. Top-down facilitation of visual recognition. *Proc Natl Acad Sci U S A*. 103:449–454.
- Bates E, Wilson SM, Saygin AP, Dick F, Sereno MI, Knight RT, Dronkers NF. 2003. Voxel-based lesion-symptom mapping. *Nat Neurosci*. 6:448–450.
- Behrmann M, Avidan G, Gao F, Black S. 2007. Structural imaging reveals anatomical alterations in inferotemporal cortex in congenital prosopagnosia. *Cereb Cortex*. 17: 2354–2363.
- Binkofski F, Buxbaum LJ. 2013. Two action systems in the human brain. *Brain Lang*. 127:222–229.
- Boronat CB, Buxbaum LJ, Coslett HB, Tang K, Saffran EM, Kimberg DY, Detre JA. 2005. Distinctions between manipulation and function knowledge of objects: evidence from functional magnetic resonance imaging. *Brain Res Cogn Brain Res*. 23:361–373.
- Bouhali F, Thiebaut de Schotten M, Pinel P, Poupon C, Mangin JF, Dehaene S, Cohen L. 2014. Anatomical connections of the visual word form area. *J Neurosci*. 34:15402–15414.
- Brandi ML, Wohlschlager A, Sorg C, Hermsdorfer J. 2014. The neural correlates of planning and executing actual tool use. *J Neurosci*. 34:13183–13194.
- Buchel C, Price C, Friston K. 1998. A multimodal language region in the ventral visual pathway. *Nature*. 394:274–277.
- Buxbaum LJ. 2017. Learning, remembering, and predicting how to use tools: distributed neurocognitive mechanisms: comment on Osiurak and Badets (2016). *Psychol Rev*. 124: 346–360.
- Canessa N, Borgo F, Cappa SF, Perani D, Falini A, Buccino G, Shallice T. 2008. The different neural correlates of action and functional knowledge in semantic memory: an fMRI study. *Cereb Cortex*. 18:740–751.
- Cant JS, Arnott SR, Goodale MA. 2009. fMR-adaptation reveals separate processing regions for the perception of form and

- texture in the human ventral stream. *Exp Brain Res.* 192: 391–405.
- Cant JS, Goodale MA. 2007. Attention to form or surface properties modulates different regions of human occipitotemporal cortex. *Cereb Cortex.* 17:713–731.
- Carey DP, Harvey M, Milner AD. 1996. Visuomotor sensitivity for shape and orientation in a patient with visual form agnosia. *Neuropsychologia.* 34:329–337.
- Carrera E, Tononi G. 2014. Diaschisis: past, present, future. *Brain.* 137:2408–2422.
- Caruana F, Avanzini P, Mai R, Pelliccia V, LoRusso G, Rizzolatti G, Orban GA. 2017. Decomposing tool-action observation: a stereo-EEG study. *Cereb Cortex.* 27:4229–4243.
- Cavina-Pratesi C, Kentridge RW, Heywood CA, Milner AD. 2010. Separate processing of texture and form in the ventral stream: evidence from fMRI and visual agnosia. *Cereb Cortex.* 20:433–446.
- Chao LL, Haxby JV, Martin A. 1999. Attribute-based neural substrates in temporal cortex for perceiving and knowing about objects. *Nat Neurosci.* 2:913–919.
- Chen Q, Garcea FE, Almeida J, Mahon BZ. 2017. Connectivity-based constraints on category-specificity in the ventral object processing pathway. *Neuropsychologia.* 105:184–196.
- Chen Q, Garcea FE, Jacobs RA, Mahon BZ. 2018a. Abstract representations of object-directed action in the left inferior parietal lobule. *Cereb Cortex.* 26:2162–2174.
- Chen L, Rogers TT. 2015. A model of emergent category-specific activation in the posterior fusiform gyrus of sighted and congenitally blind populations. *J Cogn Neurosci.* 27:1981–1999.
- Chen J, Snow JC, Culham JC, Goodale MA. 2018b. What role does “Elongation” play in “Tool-Specific” activation and connectivity in the dorsal and ventral visual streams? *Cereb Cortex.* 28:1117–1131.
- Chernoff BL, Sims MH, Smith SO, Pilcher WH, Mahon BZ under review. Direct electrical stimulation of the Frontal Aslant Tract dissociates levels of processing in sentence planning. *Cogn Neuropsychol.*
- Cohen L, Lehericy S, Chochon F, Lemer C, Rivaud S, Dehaene S. 2002. Language-specific tuning of visual cortex? Functional properties of the Visual Word Form Area. *Brain.* 125: 1054–1069.
- Creem SH, Proffitt DR. 2001. Grasping objects by their handles: a necessary interaction between cognition and action. *J Exp Psychol Hum Percept Perform.* 27:218–228.
- Culham JC, Danckert SL, DeSouza JF, Gati JS, Menon RS, Goodale MA. 2003. Visually guided grasping produces fMRI activation in dorsal but not ventral stream brain areas. *Exp Brain Res.* 153:180–189.
- Downing PE, Chan AW, Peelen MV, Dodds CM, Kanwisher N. 2006. Domain specificity in visual cortex. *Cereb Cortex.* 16: 1453–1461.
- Downing PE, Jiang Y, Shuman M, Kanwisher N. 2001. A cortical area selective for visual processing of the human body. *Science.* 293:2470–2473.
- Epstein R, Kanwisher N. 1998. A cortical representation of the local visual environment. *Nature.* 392:598–601.
- Fang F, He S. 2005. Cortical responses to invisible objects in the human dorsal and ventral pathways. *Nat Neurosci.* 8: 1380–1385.
- Fintzi AR, Mahon BZ. 2014. A bimodal tuning curve for spatial frequency across left and right human orbital frontal cortex during object recognition. *Cereb Cortex.* 24:1311–1318.
- Freud E, Macdonald SN, Chen J, Quinlan DJ, Goodale MA, Culham JC. 2017. Getting a grip on reality: Grasping movements directed to real objects and images rely on dissociable neural representations. *Cortex.* 98:34–48.
- Freud E, Plaut DC, Behrmann M. 2016. ‘What’ is happening in the dorsal visual pathway. *Trends Cogn Sci.* 20:773–784.
- Gaillard R, Naccache L, Pinel P, Clemenceau S, Volle E, Hasboun D, Cohen L. 2006. Direct intracranial, fMRI, and lesion evidence for the causal role of left inferotemporal cortex in reading. *Neuron.* 50:191–204.
- Gallivan JP, Cant JS, Goodale MA, Flanagan JR. 2014. Representation of object weight in human ventral visual cortex. *Curr Biol.* 24: 1866–1873.
- Garcea FE, Chen Q, Vargas R, Narayan DA, Mahon BZ. 2018. Task- and domain-specific modulation of functional connectivity in the ventral and dorsal object-processing pathways. *Brain Struct Funct.* 223:2589–2607.
- Garcea FE, Chernoff BL, Diamond B, Lewis W, Sims MH, Tomlinson SB, Mahon BZ. 2017. Direct electrical stimulation in the human brain disrupts melody processing. *Curr Biol.* 27:2684–2691 e2687.
- Garcea FE, Mahon BZ. 2014. Parcellation of left parietal tool representations by functional connectivity. *Neuropsychologia.* 60:131–143.
- Goebel R, Esposito F, Formisano E. 2006. Analysis of functional image analysis contest (FIAC) data with brainvoyager QX: from single-subject to cortically aligned group general linear model analysis and self-organizing group independent component analysis. *Hum Brain Mapp.* 27:392–401.
- Goodale MA, Jakobson LS, Keillor JM. 1994. Differences in the visual control of pantomimed and natural grasping movements. *Neuropsychologia.* 32:1159–1178.
- Goodale MA, Milner AD, Jakobson LS, Carey DP. 1991. A neurological dissociation between perceiving objects and grasping them. *Nature.* 349:154–156.
- Grill-Spector K, Malach R. 2004. The human visual cortex. *Annu Rev Neurosci.* 27:649–677.
- Hannagan T, Amedi A, Cohen L, Dehaene-Lambertz G, Dehaene S. 2015. Origins of the specialization for letters and numbers in ventral occipitotemporal cortex. *Trends Cogn Sci.* 19: 374–382.
- Haxby JV, Gobbini MI, Furey ML, Ishai A, Schouten JL, Pietrini P. 2001. Distributed and overlapping representations of faces and objects in ventral temporal cortex. *Science.* 293: 2425–2430.
- He C, Peelen MV, Han Z, Lin N, Caramazza A, Bi Y. 2013. Selectivity for large nonmanipulable objects in scene-selective visual cortex does not require visual experience. *Neuroimage.* 79:1–9.
- Hutchison RM, Culham JC, Everling S, Flanagan JR, Gallivan JP. 2014. Distinct and distributed connectivity patterns across cortex reflect the domain-specific constraints of object, face, scene, body, and tool category-selective modules in the ventral visual pathway. *Neuroimage.* 96:216–236.
- Hutchison RM, Gallivan JP. 2016. Functional coupling between frontoparietal and occipitotemporal pathways during action and perception. *Cortex.* 98:8–27.
- Ishibashi R, Pobric G, Saito S, Lambon Ralph MA. 2016. The neural network for tool-related cognition: An activation likelihood estimation meta-analysis of 70 neuroimaging contrasts. *Cogn Neuropsychol.* 33:241–256.
- Kanwisher N, McDermott J, Chun MM. 1997. The fusiform face area: a module in human extrastriate cortex specialized for face perception. *J Neurosci.* 17:4302–4311.
- Kastner S, Chen Q, Jeong SK, Mruczek REB. 2017. A brief comparative review of primate posterior parietal cortex: a novel

- hypothesis on the human toolmaker. *Neuropsychologia*. 105:123–134.
- Kellenbach ML, Brett M, Patterson K. 2003. Actions speak louder than functions: the importance of manipulability and action in tool representation. *J Cogn Neurosci*. 15:30–46.
- Konen CS, Kastner S. 2008. Two hierarchically organized neural systems for object information in human visual cortex. *Nat Neurosci*. 11:224–231.
- Konen CS, Mruczek RE, Montoya JL, Kastner S. 2013. Functional organization of human posterior parietal cortex: grasping- and reaching-related activations relative to topographically organized cortex. *J Neurophysiol*. 109:2897–2908.
- Konkle T, Oliva A. 2012. A real-world size organization of object responses in occipitotemporal cortex. *Neuron*. 74:1114–1124.
- Kravitz DJ, Saleem KS, Baker CI, Mishkin M. 2011. A new neural framework for visuospatial processing. *Nat Rev Neurosci*. 12:217–230.
- Kravitz DJ, Saleem KS, Baker CI, Ungerleider LG, Mishkin M. 2013. The ventral visual pathway: an expanded neural framework for the processing of object quality. *Trends Cogn Sci*. 17:26–49.
- Kveraga K, Boshyan J, Bar M. 2007. Magnocellular projections as the trigger of top-down facilitation in recognition. *J Neurosci*. 27:13232–13240.
- Levy I, Hasson U, Avidan G, Hendler T, Malach R. 2001. Center-periphery organization of human object areas. *Nat Neurosci*. 4:533–539.
- Lyon DC, Nassi JJ, Callaway EM. 2010. A disynaptic relay from superior colliculus to dorsal stream visual cortex in macaque monkey. *Neuron*. 65:270–279.
- Macdonald SN, Culham JC. 2015. Do human brain areas involved in visuomotor actions show a preference for real tools over visually similar non-tools? *Neuropsychologia*. 77:35–41.
- Mahon BZ, Anzellotti S, Schwarzbach J, Zampini M, Caramazza A. 2009. Category-specific organization in the human brain does not require visual experience. *Neuron*. 63:397–405.
- Mahon BZ, Caramazza A. 2011. What drives the organization of object knowledge in the brain? *Trends Cogn Sci*. 15:97–103.
- Mahon BZ, Kumar N, Almeida J. 2013. Spatial frequency tuning reveals interactions between the dorsal and ventral visual systems. *Journal of Cognitive Neuroscience*. 25:862–871.
- Mahon BZ, Milleville SC, Negri GA, Rumiati RI, Caramazza A, Martin A. 2007. Action-related properties shape object representations in the ventral stream. *Neuron*. 55:507–520.
- Mahon BZ, Wu W. 2015. Cognitive penetration of the dorsal visual stream? In: Zeimbekis J, Athanasios R, editors. *The cognitive penetration of perception: new philosophical perspectives*. Oxford, UK: Oxford. p. 200–217.
- Martin A. 2006. Shades of Dejerine—forging a causal link between the visual word form area and reading. *Neuron*. 50:173–175.
- Martin A. 2007. The representation of object concepts in the brain. *Annu Rev Psychol*. 58:25–45.
- Martin A, Wiggs CL, Ungerleider LG, Haxby JV. 1996. Neural correlates of category-specific knowledge. *Nature*. 379:649–652.
- Noppeney U, Price CJ, Penny WD, Friston KJ. 2006. Two distinct neural mechanisms for category-selective responses. *Cereb Cortex*. 16:437–445.
- Op de Beeck HP, Haushofer J, Kanwisher NG. 2008. Interpreting fMRI data: maps, modules and dimensions. *Nat Rev Neurosci*. 9:123–135.
- Osher DE, Saxe RR, Koldewyn K, Gabrieli JD, Kanwisher N, Saygin ZM. 2016. Structural connectivity fingerprints predict cortical selectivity for multiple visual categories across cortex. *Cereb Cortex*. 26:1668–1683.
- Osiurak F, Badets A. 2016. Tool use and affordance: manipulation-based versus reasoning-based approaches. *Psychol Rev*. 123:534–568.
- Peelen MV, Downing PE. 2007. The neural basis of visual body perception. *Nat Rev Neurosci*. 8:636–648.
- Peeters RR, Rizzolatti G, Orban GA. 2013. Functional properties of the left parietal tool use region. *Neuroimage*. 78:83–93.
- Pelli DG. 1997. The VideoToolbox software for visual psychophysics: transforming numbers into movies. *Spat Vis*. 10:437–442.
- Perenin MT, Rossetti Y. 1996. Grasping without form discrimination in a hemianopic field. *Neuroreport*. 7:793–797.
- Prentiss EK, Schneider CL, Williams ZR, Sahin B, Mahon BZ. 2018. Spontaneous in-flight accommodation of hand orientation to unseen grasp targets: a case of action blindsight. *Cogn Neuropsychol*. 1–9. doi: 10.1080/02643294.2018.1432584
- Price CJ, Devlin JT. 2004. The pro and cons of labelling a left occipitotemporal region: “the visual word form area”. *Neuroimage*. 22:477–479.
- Price CJ, Friston KJ. 2002. Degeneracy and cognitive anatomy. *Trends Cogn Sci*. 6:416–421.
- Price CJ, Warburton EA, Moore CJ, Frackowiak RS, Friston KJ. 2001. Dynamic diaschisis: anatomically remote and context-sensitive human brain lesions. *J Cogn Neurosci*. 13:419–429.
- Riesenhuber M. 2007. Appearance isn’t everything: news on object representation in cortex. *Neuron*. 55:341–344.
- Rogers TT, Hocking J, Mechelli A, Patterson K, Price C. 2005. Fusiform activation to animals is driven by the process, not the stimulus. *J Cogn Neurosci*. 17:434–445.
- Rosenbaum DA, Marchak F, Barnes HJ, Vaughan J, Slotta JD, Jorgensen MJ. 1990. Constraints for action selection: overhand versus underhand grips. In: Jeannerod. M, editor. *Attention and performance XIII: motor representation and control*. Hillsdale, NJ: Erlbaum. p. 321–342.
- Rushworth MF, Behrens TE, Johansen-Berg H. 2006. Connection patterns distinguish 3 regions of human parietal cortex. *Cereb Cortex*. 16:1418–1430.
- Sakuraba S, Sakai S, Yamanaka M, Yokosawa K, Hirayama K. 2012. Does the human dorsal stream really process a category for tools? *J Neurosci*. 32:3949–3953.
- Saygin ZM, Osher DE, Koldewyn K, Reynolds G, Gabrieli JD, Saxe RR. 2011. Anatomical connectivity patterns predict face selectivity in the fusiform gyrus. *Nat Neurosci*. 15:321–327.
- Saygin ZM, Osher DE, Norton ES, Youssoufian DA, Beach SD, Feather J, Kanwisher N. 2016. Connectivity precedes function in the development of the visual word form area. *Nat Neurosci*. 19:1250–1255.
- Schmid MC, Panagiotaropoulos T, Augath MA, Logothetis NK, Smirnakis SM. 2009. Visually driven activation in macaque areas V2 and V3 without input from the primary visual cortex. *PLoS One*. 4:e5527.
- Schwarzbach J. 2011. A simple framework (ASF) for behavioral and neuroimaging experiments based on the psychophysics toolbox for MATLAB. *Behav Res Methods*. 43:1194–1201.
- Simmons WK, Martin A. 2012. Spontaneous resting-state BOLD fluctuations reveal persistent domain-specific neural networks. *Soc Cogn Affect Neurosci*. 7:467–475.
- Sincich LC, Park KF, Wohlgenuth MJ, Horton JC. 2004. Bypassing V1: a direct geniculate input to area MT. *Nat Neurosci*. 7:1123–1128.
- Snow JC, Pettypiece CE, McAdam TD, McLean AD, Stroman PW, Goodale MA, Culham JC. 2011. Bringing the real world into

- the fMRI scanner: repetition effects for pictures versus real objects. *Sci Rep.* 1:130.
- Stasenکو A, Garcea FE, Dombovy M, Mahon BZ. 2014. When concepts lose their color: a case of object-color knowledge impairment. *Cortex.* 58:217–238.
- Stevens WD, Kravitz DJ, Peng CS, Tessler MH, Martin A. 2017. Privileged functional connectivity between the visual word form area and the language system. *J Neurosci.* 37:5288–5297.
- Stevens WD, Tessler MH, Peng CS, Martin A. 2015. Functional connectivity constrains the category-related organization of human ventral occipitotemporal cortex. *Hum Brain Mapp.* 36:2187–2206.
- Striem-Amit E, Cohen L, Dehaene S, Amedi A. 2012. Reading with sounds: sensory substitution selectively activates the visual word form area in the blind. *Neuron.* 76:640–652.
- Talairach J, Tournoux P. 1988. Co-planar stereotaxic atlas of the human brain. 3-Dimensional proportional system: an approach to cerebral imaging. New York: Thieme Medical Publishers.
- Thiebaut de Schotten M, Cohen L, Amemiya E, Braga LW, Dehaene S. 2014. Learning to read improves the structure of the arcuate fasciculus. *Cereb Cortex.* 24:989–995.
- Thomas C, Avidan G, Humphreys K, Jung KJ, Gao F, Behrmann M. 2009. Reduced structural connectivity in ventral visual cortex in congenital prosopagnosia. *Nat Neurosci.* 12:29–31.
- Tootell RB, Devaney KJ, Young JC, Postelnicu G, Rajimehr R, Ungerleider LG. 2008. fMRI mapping of a morphed continuum of 3D shapes within inferior temporal cortex. *Proc Natl Acad Sci U S A.* 105:3605–3609.
- Tsao DY, Freiwald WA, Tootell RB, Livingstone MS. 2006. A cortical region consisting entirely of face-selective cells. *Science.* 311:670–674.
- Valyear KF, Culham JC. 2010. Observing learned object-specific functional grasps preferentially activates the ventral stream. *J Cogn Neurosci.* 22:970–984.
- Yeatman JD, Rauschecker AM, Wandell BA. 2013. Anatomy of the visual word form area: adjacent cortical circuits and long-range white matter connections. *Brain Lang.* 125:146–155.